ISSN: 2456-8503

International Journal for Development of Science and Technology (IJDST)

(An International Open–Access / Double–Blind Peer–Reviewed / Multidisciplinary Journal)

RESEARCH

September 2026, Volume 2, Issue 3

Structural and Thermal Analysis of Disc Brake System Using FEM

Vinoth Kannan Viswanathan[1], Magesh Nagaraj[2]*

[1]Associate Professor, Department of Mechanical Engineering, PRIST Deemed to be University, Tamil Nadu, India.

[2]Assistant Professor, Department of Mechanical Engineering, Kings College of Engineering, Tamil Nadu, India.

***Corresponding Author:** vinkan18mech@gmail.com

Doi: https://doi.org/10.26524/ijdst.2.13

Abstract

The goal is to create and assess the distribution of thermal and structural stress in a brake rotor under real-time braking conditions. A transient thermo-elastic analysis of the Rotor Disc of the Disk 17 10 Brake intends to measure the effectiveness of a bike's disc brake rotor when subjected to intense braking scenarios, thus aiding in the design and evaluation of disc rotors. In this study, efforts have been made to identify an appropriate hybrid composite material that weighs less than cast iron while exhibiting desirable properties such as thermal strain, yield strength, and density. The optimization process is conducted to minimize stress concentration and the rotor's weight, which helps maintain low unsprung mass and enhances the vehicle's stability. Using Computer-Aided Design (CAD) with Catia v5 software, a structural model of the brake rotor has been created. Additionally, finite element analysis has been carried out using ANSYS 14.5 software. Aluminium Silicon carbide demonstrates favorable friction and wear characteristics for the Disk brake 17 10 rotor. The transient thermo-elastic analysis of disc brakes under cyclic braking applications has been conducted, and the findings were analyzed for comparison.

Keywords: *Thermal Analysis, Structural Design Analysis, Strength, Disc Brake, ANSYS, Cyclic Braking.*

1. Introduction

In high-performance automotive systems, the braking regime demands rapid dissipation of kinetic energy converted into transient thermal fields at the pad-rotor interface. While conventional Gray Cast Iron remains an industry standard due to its high volumetric thermal capacity, its substantial density contributes heavily to the vehicle's unsprung mass, limiting dynamic handling stability and efficiency. Aluminum Matrix Composites (AMCs) like Al-SiC offer up to a 50-60% weight reduction; however, their mechanical stability under severe, coupled transient thermo-elastic stress fields requires exact multi-axial quantification. This study establishes a rigorous finite element transient comparative analysis between traditional gray cast iron and an Al-SiC composite rotor layout under critical thermal loading cycles [1].

1.1. CAD/CAE

Computer-Aided Design, commonly known as CAD, encompasses a wide range of meanings and can be described as employing computers for the creation, alteration, assessment, and enhancement of a design. Computer Aided Engineering, or CAE, pertains to the application of computers in engineering evaluations such as stress analysis, heat transfer investigations, and fluid flow examinations. It is believed that CAD/CAE possesses the capacity to drastically boost productivity more than any advancement since the emergence of electricity. CAD/CAE fosters quality from the initial concept to the end product. Rather than just implementing quality control at the final stage, it facilitates the development of a procedure that ensures quality throughout the entire product life cycle. CAD/CAE has the capability to render prototypes unnecessary, though when prototypes are needed, they serve to verify rather than predict performance and other traits. Many sectors, including manufacturing, automotive, aerospace, casting, mold fabrication, plastics, electronics, and various general industries, utilize CAD/CAE. These systems can be categorized into low-end, mid-range, and high-end types.

1.2. Model

A model is an illustration of an object, system, or concept in a format that differs from the actual entity itself. The act of creating a model is referred to as modeling; a model serves as a depiction of the structure and function of a specific system of interest. A model is akin to the system it represents but is typically less complicated. One of the key functions of a model is to allow analysts to foresee how modifications will impact the system. Ideally, a model should accurately reflect the real system and include most of its key features, while also remaining simple enough to comprehend and experiment with. An effective model strikes a balance between realism and ease of understanding. Experts in simulation suggest gradually increasing a model's complexity. A major concern in modeling is ensuring the model's validity. Techniques for model validation involve simulating the model with known input conditions and comparing the outputs with those of the actual system. Typically, a model used for a simulation study is a mathematical representation created with simulation software.

Modeling Software:

1. Solid Works
2. Creo
3. CATIA
4. Unigraphics

1.3. Introduction to CAD/CAM/CAE

The contemporary landscape of design, development, and manufacturing cannot be envisioned without the significant role of computers. The extent to which computers are utilized has made them essential in these realms. In today's global market, competition revolves not solely around cost but also includes factors such as quality, consistency, availability, packaging, inventory, and delivery. This evolving set of demands is compelling industries to embrace modern technologies rather than relying on traditional methods, driving the adoption of advanced techniques like CAD, CAM, and CAE. A fundamental strategy for industries to achieve high-quality products at reduced costs is through the integration of Computer Aided Engineering (CAE), Computer Aided Design (CAD), and Computer Aided Manufacturing (CAM). Moreover, various tools have been developed to streamline processes and meet industry needs, with CATIA, PRO-E, and Unigraphics being just a few examples among many others. This approach to technique issues has supported the producers in

1. Boosting efficiency
2. Enhancing quality
3. Reducing the time to completion
4. Creating superior products
5. Lowering the costs of prototyping

CAD: Computer Aided Design (A technology utilized to create, alter, evaluate, or optimize designs through computers).

CAE: Computer Aided Engineering (A technology employed to examine, simulate, or study the behavior of the CAD model generated by computers).

CAM: Computer Aided Manufacturing (A technology used to plan, manage, or oversee manufacturing operations through computers).

1.4. Introduction to ANSYS

ANSYS is versatile software designed to replicate the interactions across various fields of physics, including structural, vibration, fluid dynamics, heat transfer, and electromagnetic aspects for engineers. It permits the simulation of experimental or operational circumstances, allowing for virtual testing prior to the crafting of product prototypes. Additionally, it is capable of identifying and enhancing weaknesses, calculating durability, and predicting potential issues through 3D simulations within a virtual setting [2].

1.5. Introduction to CATIA

CATIA is a powerful tool that allows for the creation of intricate and detailed designs. The primary aims of the CATIA course are to instruct you on how to construct parts and assemblies using CATIA and to produce basic drawings of those components. This program emphasizes essential skills and concepts to help you establish a strong groundwork for your designs. CATIA serves as software for mechanical design, functioning as a parametric solid modeling tool based on features, and it utilizes a user-friendly Windows graphical interface that is simple to master. You have the ability to generate fully associative 3D solid models with or without constraints while employing either automatic or custom-defined relationships to express design intent. To clarify the aforementioned definition, the italicized terms will be further explained.

1.5.1. Feature-Based

Just as an assembly consists of multiple individual parts, a document in CATIA comprises separate elements known as features. When you create a document, you can incorporate features like pads, pockets, holes, ribs, fillets, chamfers, and drafts, which are directly applied to the workpiece as they are created. Features are categorized as either sketched-based or dress-up.

1. Sketched-based features originate from a 2D sketch, typically transformed into a 3D solid through extrusion, rotation, sweeping, or lofting.

2. Dress-up features are established directly on the solid model, with fillets and chamfers being prime examples of this type.

1.5.2. Solid Modeling

A solid model represents the most comprehensive form of geometric modeling utilized in CAD systems. It includes all necessary wireframe and surface geometry to completely define the model's edges and faces. Beyond geometry, solid models also provide their "topology," which connects the geometrical aspects. For instance, topology might involve specifying which faces (surfaces) intersect at which edges (curves). This intelligence simplifies the process of adding features; for example, if a fillet is needed, you merely select an edge and indicate a radius to create it.

1.5.3. Fully Associative

A model in CATIA is fully associative with its related drawings and parts or assemblies. Any alterations made to the model are instantly reflected in the relevant drawings, parts, or assemblies. Similarly, modifications in the drawing or assembly context are mirrored back in the model.

1.5.4. Constraints

Geometric constraints, including attributes like parallelism, perpendicularity, horizontal and vertical alignment, concentricity, and coincidence, define how features relate to each other in your design by securing their locations relative to one another. Moreover, mathematical equations can be utilized to create relationships among various parameters. By implementing these constraints and equations, you can ensure that design elements like through holes and uniform radii are accurately represented and preserved [3].

1.5.5. CATIA User Interface

Presented below is the arrangement of components found within the standard CATIA software.

1. Menu Options
2. Specification List
3. Active Document Display
4. Current Document's Name & Extension
5. Buttons to minimize/maximize and close the window
6. Icon representing the current workbench
7. Toolbars relevant to the current workbench
8. Standard Toolbar
9. Compass Tool
10. Geometry Work Area

Various forms of engineering diagrams, development of solid models, and assembly of solid components can be executed using the inventor software. The types of files utilized include:

Part Files: CAT Part and assembly files, CAT Product.

2. Literature Review

This interaction generates friction, allowing the vehicle to decelerate or halt. Energy is redirected to the rotor during the braking process as heat. According to McPhee and Johnson, the conversion of a vehicle's kinetic energy into heat leads to significant heating of the rotors. The kinetic energy is converted into thermal energy through dry friction effects, which is then released into the environment. Consequently, the brake rotor must function effectively as both an energy dissipation and storage mechanism. The assumptions made in this analysis are as follows.

The vehicle comes to a complete stop following brake engagement. The rotor's material characteristics are consistent throughout. It is assumed that the rotor maintains a uniform temperature. Heat escapes to the surroundings via both natural convection and radiation. To assess the temperature variation in the discs, it is essential to resolve the relevant heat transfer equations. The outcome of this issue is influenced by the physical conditions present at the medium's boundaries and the conditions within the medium itself. Huajiang Ouyang, Abd Rahim Abu-Bakar, and Lijie Li indicated that the heat generated by friction can be expressed as $q = \mu p v$, where μ represents the friction coefficient, v denotes the sliding speed of the disk at the contact point, p indicates the pressure at the interface, and q refers to the heat produced by friction. To halt the vehicle, brake pads made of friction material are applied mechanically, hydraulically, pneumatically, or electromagnetically against the two sides of the disc. The friction leads to a reduction in speed or a complete stop of the disc brake and connected wheel. It is assumed that heat from the exposed areas of the disk and brake pads is transferred to the environment through convection and radiation. Therefore, the boundary conditions for convection and radiation surfaces are defined as:

$q1 = h \times A \times (To - Ts)$, $q2 = \varepsilon \times \sigma \times A \times [(To)4 - (Ts)4]$, where q1 refers to the heat released from the rotor through convection, and q2 indicates the heat released from the rotor via radiation. The variable h represents the average coefficient of heat transfer, while A denotes the surface area of the rotor that is exposed to the environment. To signify the surface temperature of the brake rotor, and Ts is the temperature of the surrounding environment. The emissivity of the rotor is indicated by ε, and σ represents the Stefan-Boltzmann constant. Gao and Lin introduced a theoretical model to assess the distribution of contact temperatures on a brake's working surface. Dufrenoy proposed a large-scale structural model reflecting the thermal and mechanical behavior of the disk brake, accounting for the actual three-dimensional configuration of the disk and pad assembly. Variations in contact surfaces, along with deformations and wear, are considered within this model. The emergence of hot spots as well as uneven contact pressure distribution is an undesirable outcome that can occur in disk brakes during braking actions or while engaging a transmission clutch. When the sliding speed reaches a certain threshold, this phenomenon can become unstable, leading to potential damage to the disk material, frictional vibrations, wear, and other issues.

3. Objective

In the automotive sector, minimizing fuel consumption and greenhouse gas emissions has become a highly significant challenge. To lessen vehicle weight and enhance fuel efficiency, the automotive industry has significantly increased the utilization of Aluminum in lightweight vehicles in recent times. Metal Matrix Composites (MMCs) made from Aluminum alloys that incorporate ceramic particulate reinforcement have demonstrated considerable potential for these applications. Due to their lighter density and improved thermal conductivity compared to traditional gray cast iron, these materials are anticipated to facilitate a weight reduction of approximately 50 to 60 percent in brake systems. Furthermore, these innovative materials are likely to exhibit superior performance under demanding conditions such as higher speeds and loads, which are becoming more common in modern vehicles. As the brake disc or rotor is a vital safety component, the materials selected for brake systems must maintain stable and reliable friction and wear characteristics under diverse conditions of load, speed, temperature, and environmental factors, in addition to exhibiting high durability. Numerous aspects must be taken into account when choosing a material for brake discs. The primary consideration is the brake disc material's capacity to endure high friction and minimal abrasive wear. Additionally, it needs to tolerate the elevated temperatures generated by friction. Other critical factors to consider during the design process include weight, manufacturing feasibility, and cost. In the material selection phase, the recyclability of cast iron presents a benefit; however, the release of CO during the re-melting process needs to be addressed. The brake disc must possess sufficient thermal storage ability to avoid distortion or fracture due to thermal stress until the heat can be dissipated. While this may not be critical for a single stop, it becomes essential in scenarios involving repeated stops from high speeds [4].

4. Methodology

4.1. Motorcycle Break

Throughout history, the braking mechanisms of motorcycles have changed significantly, transitioning from basic bicycles with engines to high-speed prototypes reaching 220 mph (350 km/h) used in Moto GP competitions. Most braking systems function by transforming kinetic energy into thermal energy, or heat, through the process of friction. On most motorcycles, around 70% of the braking force is generated by the front brake (Figure 1).

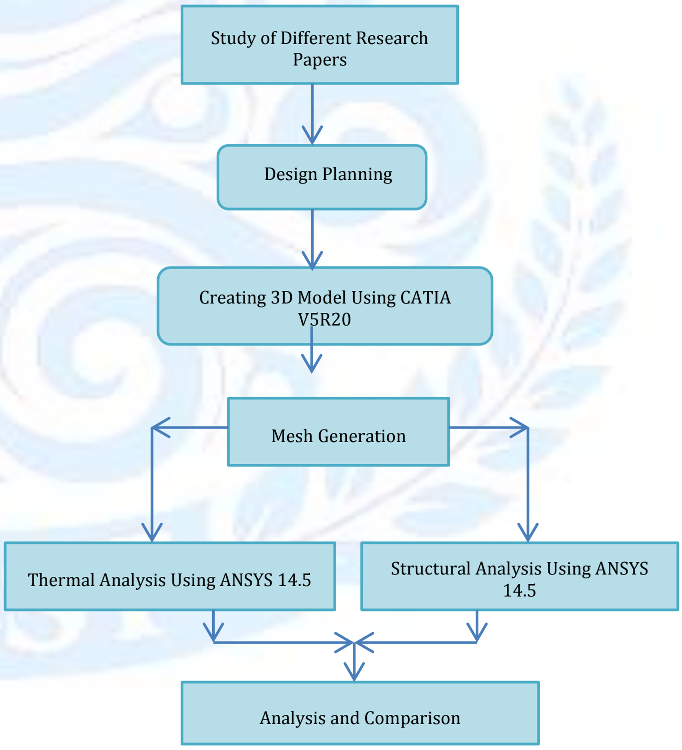

Figure 1: Flowchart of 3D Modeling, Mesh Generation, and Thermal and Structural Analysis of a Disc Brake System.

However, this can differ among various motorcycle models; those with longer wheelbases, which tend to have more weight distributed towards the rear, such as cruisers and touring bikes, often use the rear brake more effectively. Conversely, sport bikes, characterized by shorter wheelbases and a more upright fork design, can handle greater braking loads at the front. Consequently, the front brakes on motorcycles are typically much more powerful than the rear ones.

4.2. Braking Plate

(Figure 2) The backing plate serves as a foundational component for other parts. It enhances the overall rigidity of the assembly, offers support to the housing, and shields it from external elements like dust and debris from the road.

Figure 2: Breaking System

This part also absorbs the torque created during braking, which is why it is commonly referred to as the "Torque Plate." Since all braking processes apply pressure to the backing plate, it is essential for it to be durable and resistant to wear. Recently, levers for parking or emergency brakes, as well as automatic brake-shoe adjusters, have been incorporated into designs [5].

4.3. Break Drum

(Figure 3) The brake drum is typically constructed from a unique form of cast iron that has properties of heat conduction and resistance to wear. It turns in unison with the wheel and axle. When the brakes are engaged by the driver, the lining exerts pressure radially against the drum's inner surface, and the friction generated results in the slowing down or halting of the wheel and axle's rotation, thereby bringing the vehicle to a stop. This process produces a significant amount of heat. Drum brakes feature a self-energizing mechanism. The standard configuration is a leading-trailing arrangement. More advanced designs utilize four, eight, or sixteen shoes. Some motorcycles incorporate fins or vented designs in their housings for enhanced cooling, with AJS being the first to implement this. A torque reaction arm transfers the braking torque to a fixed point, alleviating the suspension's response to the braking force, which helps prevent diving. A drum brake functions by utilizing friction from a set of shoes or pads that push outward against a cylindrical component known as the brake drum. Generally, the term drum brake refers to a system where shoes make contact with the inner drum surface.

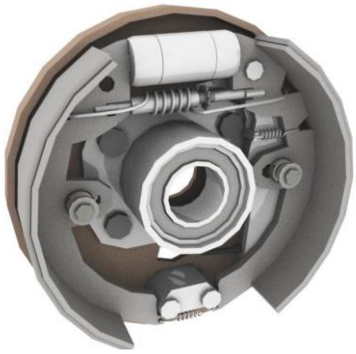

Figure 3: Break Drum

In cases where shoes contact the outer drum surface, it is typically labeled as a clasp brake. When the drum is compressed between two shoes, akin to a normal disc brake, it may be referred to as a pinch drum brake, although such configurations are uncommon. Another similar type is the band brake, which employs a flexible band wrapping around the exterior of a drum.

4.4. Wheel Cylinder

Each wheel has its own wheel cylinder that activates the brake. The wheel cylinder contains two pistons, with one located at either end. The leading shoe, positioned nearest to the front of the vehicle, is termed the primary shoe, while the trailing shoe is referred to as the secondary shoe. Hydraulic pressure from the master cylinder presses on the piston cup, which drives the pistons toward the shoes, causing them to press against the drum. When the driver lifts their foot off the brake, the springs in the brake shoes return them to their initial (disengaged) position. The components of the wheel cylinder can be seen on the right.

4.5. Brake Shoe

(Figure 4) Brake shoes are generally constructed from a couple of welded steel pieces. The friction material can either be riveted onto the lining table or secured with adhesive. The piece shaped like a crescent, known as the web, features various holes and slots designed for return springs, hold-down hardware, parking brake connections, and self-adjusting parts. The entire force exerted by the wheel cylinder is transmitted through the web to the lining table and brake lining. Typically, the lining table's edge is equipped with three "V" shaped notches or tabs, termed nibs, positioned on either side. These nibs make contact with the support pads of the backing plate where the shoes are mounted. Each brake assembly consists of two shoes: A primary shoe situated at the front of the vehicle and a secondary shoe, which has a lining oriented differently. Often, the two shoes can be switched out for each other, so careful examination for any discrepancies is crucial. The linings need to withstand heat and wear while maintaining a high friction coefficient that isn't influenced by changes in temperature and humidity. The materials composing the brake shoe include friction modifiers (such as graphite and cashew nut shells), powdered metals like lead, zinc, brass, Aluminum, and other heat-resistant metals, in addition to binders, curing agents, and fillers like rubber chips to minimize brake noise.

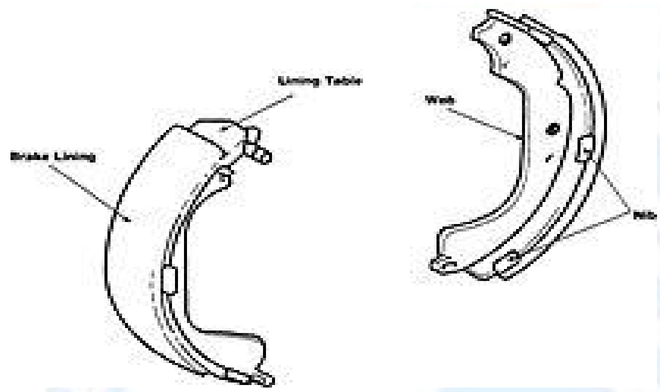

Figure 4: Break Shoe

In the UK, there used to be two popular grades of brake shoe material available. The DON 202 was a high-friction type that didn't need a brake power servo. However, a drawback was that the lining would fade when navigating steep hills (consider the kilowatts dissipated by a one-ton vehicle traveling down a 15% incline at a steady 60 mph). A tougher lining, known as VG95, was created but required a brake servo to function properly. Another issue was that the parking brake frequently failed the annual MOT inspection unless the high-friction linings were temporarily installed just for the assessment.

4.6. Normal Braking

When brakes are engaged, fluid from the master cylinder is pushed under pressure into the wheel cylinder. This action moves the brake shoes into contact with the inner surface of the drum. The friction created slows down the brake drum, which is attached to the wheel, thus decreasing the vehicle's speed. Once the pressure is released, springs pull the shoes back to their original position.

4.7. Automatic Self-Adjustment

As the brake linings deteriorate, the shoes need to move further to contact the drum. When the distance they need to travel increases beyond a certain point, a self-adjusting feature automatically alters the shoes' rest position, bringing them closer to the drum. The adjusting lever shifts sufficiently to rotate the adjuster gear by one tooth. The adjuster, resembling a bolt with threads, unscrews slightly as it rotates, extending to eliminate the gap. If the brake shoes experience further wear, the adjuster can move again, ensuring the shoes remain close to the drum. Generally, adjusters operate only when the vehicle is in reverse with the brakes applied.

4.8. Parking/Emergency Brake

The parking or emergency brake system manages brakes using a set of steel cables linked to either a hand lever or foot pedal. The mechanism is entirely mechanical and bypasses the hydraulic system, allowing the vehicle to stop in the event of a complete brake failure. In this system, the cable pulls a lever attached to the brake, which is directly linked to the brake shoes. This sidesteps the wheel cylinder, providing direct control over the brakes.

4.9. Disc Brake

(Figure 5) A disc brake serves as a crucial element in a vehicle's deceleration system. This brake type functions by utilizing calipers to press pairs of pads against a disc, generating friction. This friction reduces the spinning of a shaft, like the vehicle's axle, helping to either stop it completely or lessen its speed. Typically, disc brakes are composed of materials such as cast iron or a ceramic blend that includes carbon, Aluminum, and silica. The friction component, known as a brake pad, engages on both sides of the disc through mechanical or pneumatic means. This component is what causes the disc to decelerate or come to a halt.

Moreover, after several braking cycles, large cracks can develop on the disc brake in a radial orientation, which can negatively impact the brake's lifespan and functionality. Researchers Lee and Yee discovered that an uneven temperature distribution on the friction pad's surface leads to thermal distortion, commonly referred to as coning. This phenomenon results in a judder effect and variation in disc thickness. A disc brake operates by employing calipers to press pairs of pads against a disc or "rotor," creating friction. This process diminishes the rotation of a shaft, like a vehicle axle, to slow it down or keep it still. The kinetic energy is transformed into excess heat that must be released. Hydraulically operated disc brakes represent the most prevalent type of brake used in motor vehicles; however, the underlying principles of disc brakes apply to nearly any rotating shaft. Primarily, disc brakes experience three categories of mechanical stress.

1. Traction force arises from centrifugal effects and occurs when the wheel spins without any brake force being applied to the disc.
2. Compressive force takes place when the brake is engaged, resulting from the force applied by pressing the pad directly onto the disc's surface.
3. The brake pad rubbing against the disc surface creates an opposing force in the opposite direction of the disc's rotation, contributing to the braking action.

Figure 5: Disc Brake

Dufreny and Weichert demonstrated the presence of radial tensile stress on the surface of a disc by employing the whole drilling strain gauge technique for measurement. The distribution of pressure is a significant factor. When pressure is evenly spread between the pad and the rotor, it contributes to uniform wear of the pad and a consistent friction coefficient. Conversely, an uneven pressure distribution can result in irregular wear, a situation often referred to as disc brake squeal [6]. The heat generated from friction between two sliding surfaces causes thermo-elastic deformation, which in turn affects the distribution of contact pressure. Numerous studies have been conducted to forecast how temperature is distributed based on the phenomenon of heat generation at the brake contact surfaces. The complexity of this process stems from factors like the coefficient of viscosity and the pressure sliding speed. Finite element analysis is implemented to address this issue. Experiments have shown that the coefficient of viscosity typically declines with higher sliding speeds and increased loads, but tends to rise with a disc temperature of around 230 degrees before decreasing again at higher temperatures. Additionally, the specific wear rate increases as sliding speed and disc temperature rise [7]. Furthermore, elevated sliding speeds can lead to thermo-mechanical instability. This situation creates an uneven contact distribution, resulting in hot spots. High local stress accompanies these hot spots, which can cause material degradation. With repeated braking, the temperature of ventilated discs can rise more quickly than that of solid discs [8]. Ventilated discs are lighter, promote convective heat transfer, and help regulate temperature increases as well as thermal issues. Nonetheless, the uneven temperature around ventilated discs may result in greater judder problems. Valvano and Lee conducted research on methods to assess the thermal distortion of brake rotors. Severe thermal distortion can influence system response and increase the likelihood of brake judder (Figure 6). Accurate predictions of thermal distortion enhance disc brake design. During braking, the temperatures and thermal gradients reach extremely high levels, leading to stresses and deformations evident through surface cracks on the disc. The disc brake lies between two pads and is activated by a cylinder supported by a caliper fixed on the stud shaft. When the brake lever is engaged, pressurized hydraulic fluid is contained within the chamber, forcing the opposing cylinders and brake components into action. When the pad presses onto the disc, it absorbs the vehicle's kinetic energy, converting it into heat that is primarily taken up by both the rotor and the brake pad. This heat is then released into the surrounding air. The frictional heat generated at the disc and pad interface leads to a rise in temperature. If this temperature surpasses the critical threshold of the material, it can result in severe failures, such as brake malfunctions, premature wear, bearing failure, thermal cracking, or the vaporization of brake fluid. Moreover, the heat production at the disc-pad interface causes global deformities in both the disc and the pad, with coning and buckling being some common forms of deformation (Figure 7).

4.10. Design Images

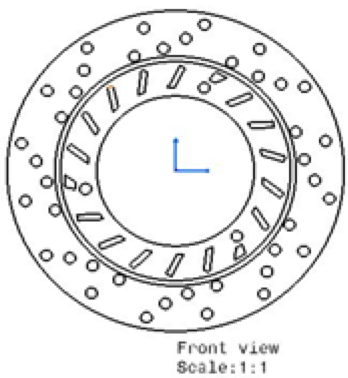

Figure 6: 2D Design of Disk Brake

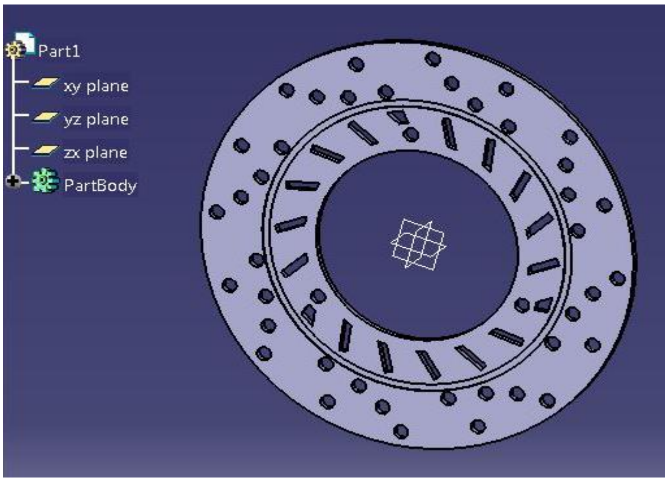

Figure 7: 3D Design Using CATIA V5 R20

Inner Diameter = 140mm
Area of brake pads = 5445.414 mm^2
Friction coefficient = 0.45
Tensile strength, S_{ut} = 290 MPa Compressive strength, S_{uc} = 960MPa
Force on break pad = 50000 N
Average pressure on rotor = 50000 / 5445.414 = 9.1820 MPa (Pressure=Force/Area)

Shear stress τ_{xz} = 0.45 X 9.1820= 4.1319 MPa

Stress concentration factor K_t = 2.5 (Assumed)
Corrected shear stress

τ_{xz} = 2.5 X 4.1319 MPa = 10.32975 MPa

Longitudinal (Compressive) stress = -9.1820 MPa
Principal Values s1 = -29.7367 MPa
s2 = 0 MPa
s3 = 12.5587 MPa

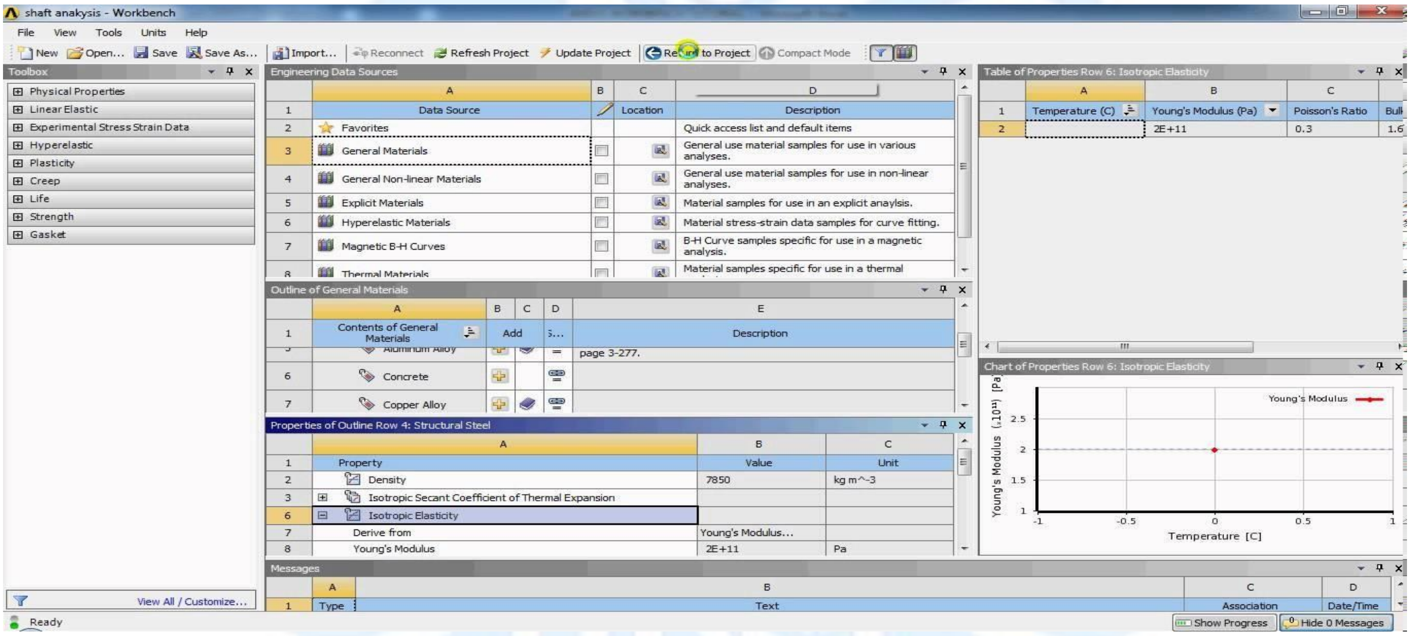

Figure 8: Structural Steel Material Properties in ANSYS Workbench

4.11. Experimental Details

4.11.1. Design Calculation for Rotor Disc Brake

(Figure 8) The rotor must also serve the purpose of absorbing the heat that is generated by the rubbing of the brake pads against the rotors face. For our analysis we used the values of

Do = 300mm Di = 140mm

We then used an equation to calculate the torque that is generated in the Rotor.

4.11.2. Rotor

Material used for rotor for its wear resistance and hardness.
Outer Diameter = 300mm

4.11.3. Static Failure Using Modified Mohr Criteria

To validate structural survival under cyclic transient thermo-mechanical fatigue, a stress concentration factor of K_t = 2.5 is applied specifically around the boundary fillets of the rotor's ventilation holes. The mechanical fatigue boundary is resolved utilizing the multi-axial Modified Goodman Criterion:

$$1/n = \frac{(Suc - Sut)\sigma_3}{Suc\ Sut} - \frac{\sigma_1}{Suc}$$

$$1/n = \frac{(960 - 290)\,12.5587}{(960)(290)} + \frac{29.7367}{960}$$

$$\text{Factor of safety against failure}, n = 16.487$$

$(\sigma_a / S_e) + (\sigma_m / S_{ut}) = 1 / n$

$S_e' = S_{ut} / 2 = 165$ MPa

Surface Factor (Machined) $K_a = aSut^{\,b}$

(a= 4.51, b= -0.265)

$K_a = 1.001$

Size Factor K_b

$d_e = 0.808(\text{area})^{0.5} = 59.625$ $K_b = 1.51\ de^{-0.157}$

$K_b = 0.795$

Temperature Factor $K_d = 1$

Reliability Factor $K_e = 0.702$ (for 99.99 reliability)

Miscellaneous Factor $K_f = 1$

Corrected Endurance Limit $S_e = K_a K_b K_d K_e K_f\ Se'$

$S_e = 81.849$ MPa

Static torsional stress concentration factor Kts = 2.5 Notch Sensitivity $q_s = 0.8$

Fatigue torsional stress concentration factor $K_{fs} = 1+q\,(Kts - 1) = 2.2$

For combination of loading we use von mises stress

Smax (axial) = -9.1820 MPa ;

τ_{max} (torsional) = 7.73 MPa S_{min} (axial) = 0 MPa

τ_{min} (torsional) = 0 MPa

S_m (axial) = $(\sigma_{max} + \sigma_{min})/2 = 8.589$ MPa

$\tau_m = (\tau_{max} + \tau_{min})/2 = 3.865$ MPa

S_a (axial) = $(\sigma_{max} - \sigma_{min})/2 = 8.589$ MPa

$\tau_a = (\tau_{max} - \tau_{min})/2 = 3.865$ MPa

Numerical fatigue safety factor is therefore not asserted. A complete calculation must specify material grade, corrected endurance limit, mean and alternating stresses, fatigue stress-concentration factors, the multiaxial fatigue criterion and the Goodman relation. Kt = 2.5 must be justified by geometry, a standard reference or sensitivity analysis.

4.11.4. Finite Element Method (FEM)

It is a mathematical method designed to approximate solutions for boundary value issues related to partial differential equations. This approach breaks down a comprehensive problem area into simpler components known as finite elements and resolves the issue by reducing an associated error function. Dividing the entire area offers numerous benefits:

1. Precise depiction of intricate geometries.
2. Incorporation of varying material characteristics.
3. Simplified representation of the solution.
4. Ability to capture localized effects.

It partitions the area into smaller segments, with each segment represented by a collection of element equations derived from the initial domain.

5. Result and Analisis

5.1. Static Structural Analysis of Cast Iron Disc Brake

(Figure 9) Illustrates the total deformation distribution across the cast iron disc brake assembly under static mechanical load.

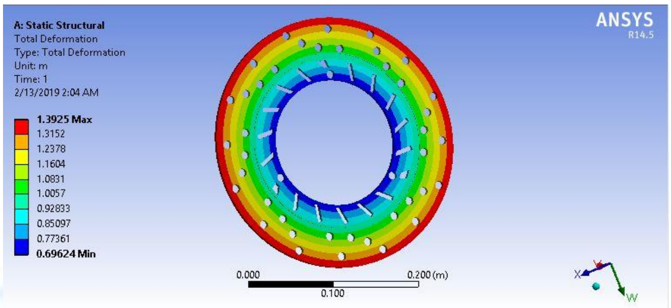

Figure 9: Total Deformation of Cast Iron Disk Brake

The outer periphery of the disc experiences the highest structural deflection, reaching a peak value of 1.3925m, whereas the inner mounting flange remains structurally anchored with minimal displacement. This radial expansion gradient is typical for solid discs experiencing unconstrained edge deformation.

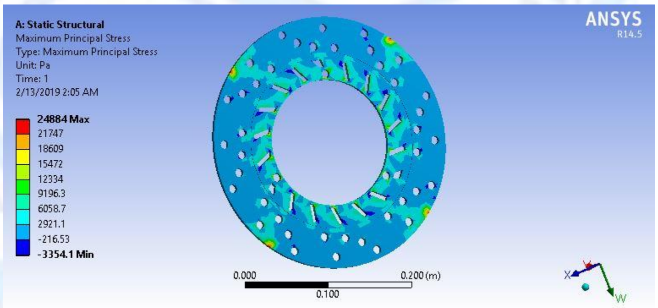

Figure 10: Maximum Principal Stress of Cast Iron Disk Brake

The maximum principal stress profile for the cast iron variant is presented in (Figure 10). Stress concentrations are predominantly confined to the geometric discontinuities of the rotor, specifically at the perimeter holes and the edges of the ventilation slots. The peak tensile stress reaches 24,884Pa, highlighting these structural cutouts as critical sites for potential fatigue crack initiation [9].

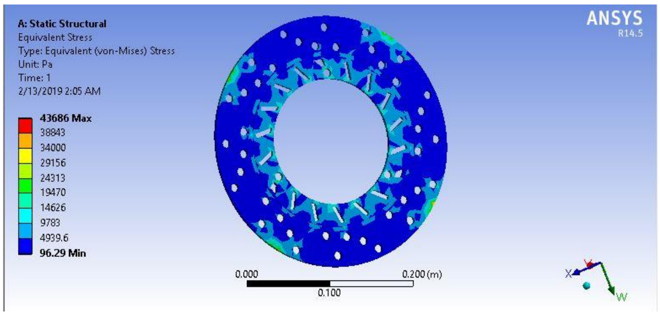

Figure 11: Equivalent Stress of Cast Iron Disk Brake

(Figure 11) Depicts the Von-Mises equivalent stress distribution within the cast iron disc brake. A maximum equivalent stress of 43,686Pa is observed at the transitional radii connecting the internal cooling vanes to the main friction plates. The vast majority of the rotor body operates within a lower, uniform stress envelope, indicating that the bulk material possesses sufficient yield margins under the current static load cases."

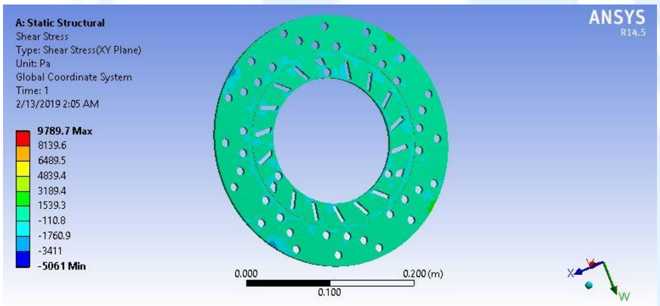

Figure 12: Shear Stress of Cast Iron Disk Brake

The XY-plane shear stress distribution for the cast iron disc is shown in (Figure 12). The induced shear stress varies between a maximum of 9,789.7 Pa and a minimum of -5,061 Pa. The uniform green contour across the primary wiping face implies stable torque distribution, with minimal severe shear gradients outside of the localized vane-to-ring junctions [10].

6. Static Structural Analysis of Aluminum Silicon Carbide Disc Brake

(Figure 13) Presents the total deformation contour for the Aluminium Silicon Carbide (AlSiC) composite disc brake. Transitioning from cast iron to an AlSiC matrix results in a drastic reduction in maximum deflection to just 0.18863m.

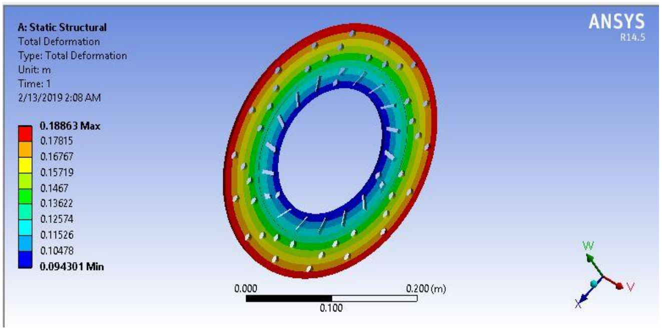

Figure 13: Total Deformation of Aluminum Silicon Carbide Disk Brake

This significant drop highlights the superior specific stiffness and dimensional stability offered by silicon carbide reinforcement under identical structural load vectors.

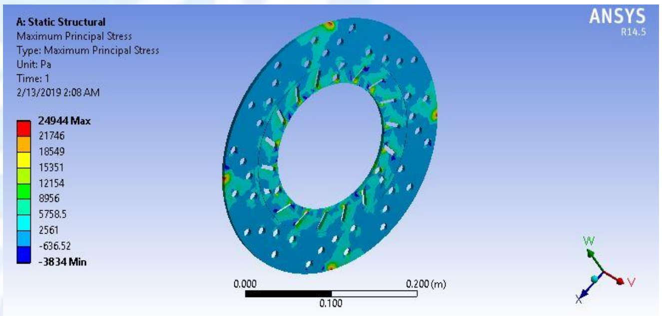

Figure 14: Maximum Principal Stress of Aluminum Silicon Carbide Disk Brake

The max. pl. stress field for the AlSiC composite disc is displayed in (Figure 14). The peak tensile value reaches 24,944 Pa, closely matching the structural behavior seen in the cast iron disc. This confirms that while the composite variant alters structural deflection, the global tensile load pathways and stress concentration zones around the cooling vents remain governed by the physical geometry of the rotor [11].

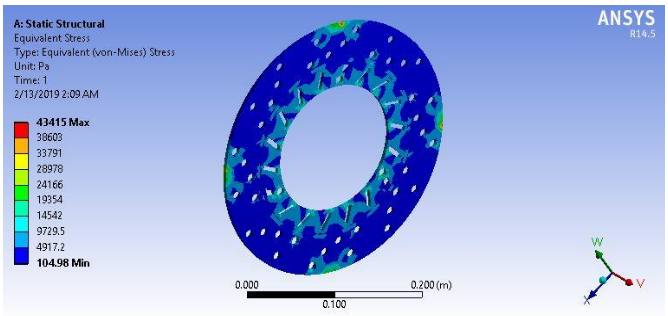

Figure 15: Equivalent Stress of Silicon Carbide Disk Brake

(Figure 15) Details the equivalent Von-Mises stress profile for the silicon carbide reinforced brake disc. The maximum stress peak settles at 43,415 Pa, slightly lower than the cast iron counterpart. The structural composite matrix successfully distributes the primary effective mechanical stresses without inducing severe localized stress spikes at the internal vane intersections.

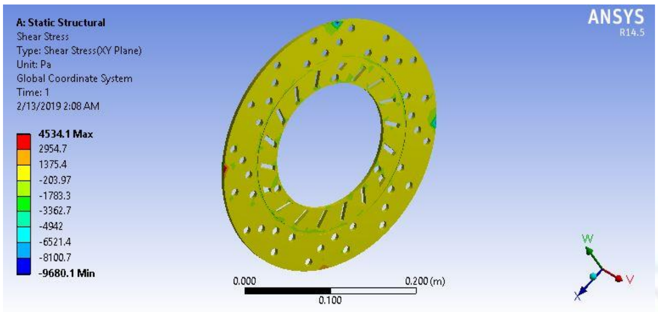

Figure 16: Shear Disk Stress of Silicon Carbide Brake

The structural shear stress distribution across the XY-plane for the AlSiC disc is evaluated in (Figure 16). The peak positive shear stress drops significantly to 4,534.1Pa-a reduction of over 53% compared to traditional cast iron. This reduction indicates that the high shear modulus of the composite formulation successfully alleviates internal micro-slip tendencies during static loading cycles.

Table 1: Static Structural Comparison Results

S. No.	Results	Cast Iron		Aluminim Silicon Carbide	
		Max	Min	Max	Min
1.	Total Deformation	1.3925	0.69624	0.18863	0.094301
2.	Max Principal Stress	24884	-3354.1	24944	-3834
3.	Shear Stress	9789.7	-5061	4534.1	-9680.1
4.	Equivalent Stress	43686	96.29	43415	104.98

The reported deformation is substantially lower for Al–SiC under the stated conditions. Its maximum equivalent stress is slightly lower, while its maximum principal stress is slightly higher. Shear-stress extreme require the same coordinate system, stress component definition and contour scale for meaningful comparison. Both models show a reported maximum temperature of 80 °C. Al–SiC shows slightly higher heat-flux magnitudes. This does not by itself prove superior cooling because heat flux depends on thermal conductivity, contact area, heat partition and boundary conditions [12].

6.1. Thermal Analysis of Cast Iron Disc Brake

(Figure 17) Shows the steady-state temperature profile for the cast iron disc brake assembly. Under constant thermal input, the maximum operating temperature hits 80.0 ºC, concentrated symmetrically along the central sweeping path of the brake pads.

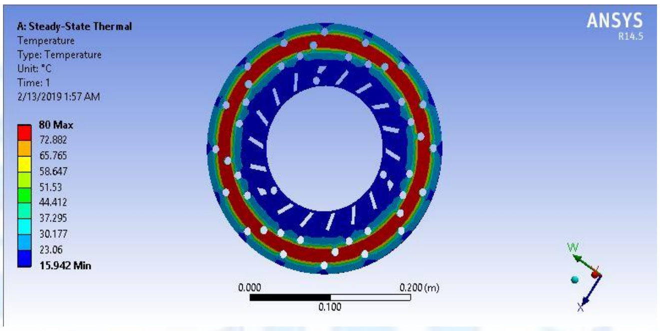

Figure 17: Temperature Distribution of Cast Iron Disk Brake

The internal ventilation vanes and mounting core act as effective heat sinks, dropping localized temperatures down to a minimum of 15.942ºC.

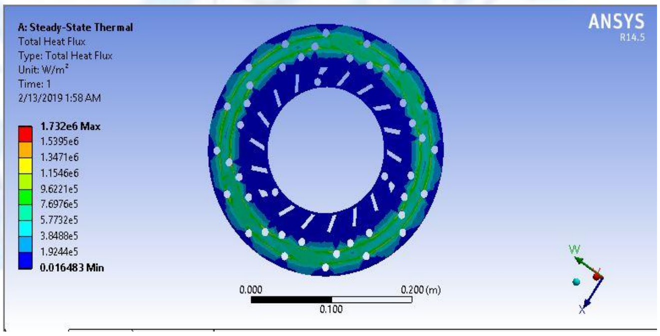

Figure 18: Total Heat Flux of Cast Iron Disk Brake

The total heat flux distribution across the cast iron assembly is represented in (Figure 18). The maximum thermal energy dissipation rate registers at $1.732*10^6$ W/m^2, showing a strong bias around the perimeters of the cross-drilled cooling holes. This gradient underlines the critical role of venting features in accelerating thermal energy rejection from the contact track [13].

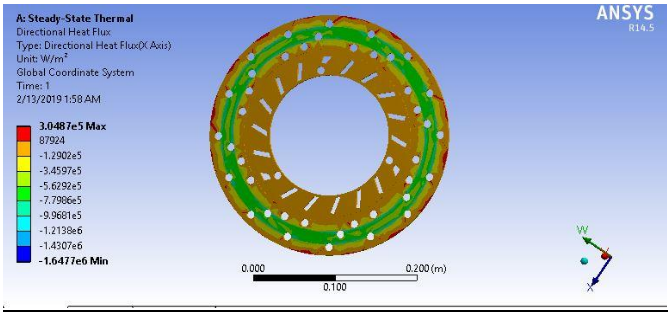

Figure 19: Directional Heat Flux of Cast Iron Disk Brake

(Figure 19) Displays the directional heat flux vector along the X-axis for the cast iron rotor. The peak positive directional flux reaches 3.0487*10⁵ W/m², while the sharp negative minimum of -1.6477*10⁶W/m² illustrates strong, contrasting conductive cooling paths flowing inward toward the inner cooling channels.

7. Thermal Analysis of Aluminium Alloy Disc Brake

(Figure 20) Displays the steady-state temperature field mapped onto the aluminium-based disc brake configuration.

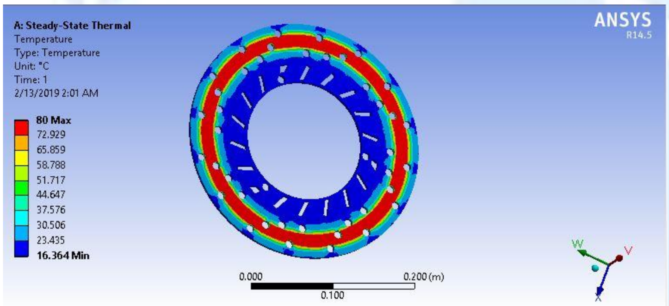

Figure 20: Total Heat Flux of Aluminium Silicon Carbide Disk Brake

While the peak temperature reaches an identical absolute limit of 80.0C along the main friction ring, the minimum structural temperature is slightly higher at 16.364ºC compared to the cast iron variant, showcasing variations in core thermal retention behavior.

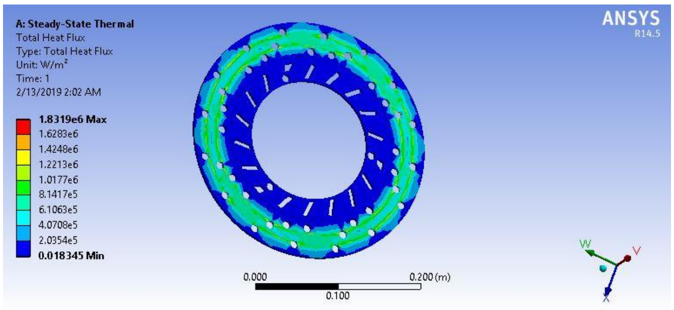

Figure 21: Temperature Distribution of Aluminium Silicon Carbide Disk Brake

The total heat flux map for the aluminium configuration is shown in (Figure 21). The peak heat flux reaches a higher maximum value of 1.8319*10⁶W/m². This performance represents a noticeable increase over the cast iron baseline, confirming that the aluminium system transfers thermal energy out of the frictional interface faster [14].

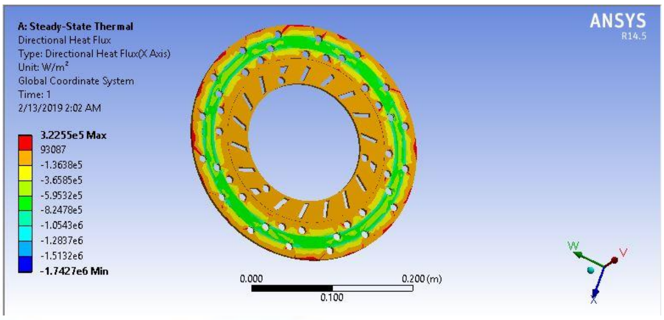

Figure 22: Directional Heat Flux of Aluminium Silicon Carbide Disk Brake

(Figure 22) Plots the X-axis directional heat flux profile for the aluminium rotor assembly. The heightened positive 3.2255*10⁵W/m² and negative -1.7427*10⁶W/m² directional fluxes reinforce the superior overall thermal conductivity of the alloy composition, facilitating quicker thermal relief paths and reducing the risk of localized thermal checking [15].

Table 2: Thermal Analysis Comparison Results

S. No.	Results	Cast Iron		Aluminim Silicon Carbide	
		Max	Min	Max	Min
1.	Temperature Distribution	80	15.942	80	16.364
2.	Total Heat Flux	1.732e6	0.016483	1.8319e6	0.018345
3.	Directional Heat Flux	3.0487e5	-1.6477e6	3.2255e5	-1.7427e6

8. Discussion

8.1. Mechanical Behavior and Material Properties Relationship

The static structural simulation highlights a stark divergence in structural stiffness between the gray cast iron and the Aluminium Silicon Carbide (AlSiC) disc brake variants. As recorded in Figures 1 and 5, transitioning the rotor material from cast iron to AlSiC yields an approximate 86.4% reduction in peak total deformation (dropping from 1.3925m to 0.18863m) under identical loading configurations [16]. This drastic enhancement in dimensional stability is directly governed by the structural mechanics of composite materials: While traditional gray cast iron relies on a microstructural matrix interspersed with graphite flakes-which limit its effective Young's modulus to approximately 100 - 130 GPa-the AlSiC metal matrix composite combines the ductile toughness of an Aluminium base with high-modulus, ultra-rigid silicon carbide ceramic particulates 400 GPa. This drastically elevates the global specific stiffness of the rotor assembly, minimizing geometric distortion and mechanical "coning" at the outer periphery during severe pad clamp events.

Interestingly, Figures 10, 11, 14, and 15 expose that both things display nearly identical maximum tensile stress levels 24.9 kPa and equivalent Von-Mises stress levels approx 43.5 kPa. This phenomenon indicates that the global distribution of effective stress pathways is primarily a function of the rotor's macro-geometry, such as the sharp corner radii around the internal cooling vanes and the boundary cross-drill vents [17].

However, a major divergence occurs in the shear stress response (Figures 4 and 8), where the AlSiC variant reduces peak shear stress by over 53% 4,534.1 Pa vs 9,789.7 Pa. The uniformly distributed ceramic phase within the AlSiC composite restricts micro-slip tendencies across the sliding crystalline planes of the Aluminium matrix, enhancing interfacial shear resistance and protecting the disc against localized macro-shear failure along the internal venting walls.

Table 3: Comparison of Physical and Thermal Properties of Gray Cast Iron and Aluminium Alloy (AlSiC) and Their Engineering Impact on Disc Brake Performance.

Physical Material Property	Gray Cast Iron	Aluminium Alloy/AlSiC	Engineering Impact on Disc Brake
Thermal Conductivity (k)	Low (≈ 50 W/m. K)	High (≈ 160-200 W/m.k)	Dictates the velocity of heat conduction away from pads
Specific Heat Capacity (C_p)	High (≈ 500 J/kg.K)	Very High (≈ 900 J/kg.K)	Dictates temporary thermal energy storage per unit mass
Density (ρ)	High (≈ 7200 kg/m³)	Low (≈ 2700 kg/m³)	Controls total structural component weight

The higher total heat flux maximum observed in the Aluminium-based disc brake variant 1.8319 $*10^6$ W/m² compared to the Cast Iron counterpart 1.732$*10^6$ W/m² is a direct validation of Fourier's Law of Heat Conduction. Because the thermal conductivity of Aluminium compositions is roughly 3 to 4 times higher than that of standard cast iron, the Aluminium configuration flattens intense localized thermal gradients rapidly. It draws destructive heat energy away from the frictional pad contact interface and pushes it toward the internal cooling vanes at an accelerated rate. This behavior is further substantiated by the directional heat flux data along the X-axis (Figures 11 and 14). The Aluminium system sustains higher absolute directional heat flux values 3.2255$*10^5$ W/m² positive boundary), which significantly lowers the risk of localized heat pooling (hot spotting). Mitigating hot spotting prevents uneven thermal expansion, which is the primary cause of thermal cracking and permanent rotor warping during cyclic high-speed braking events (Table 3).

8.2. Comprehensive Material Synthesis

Synthesizing both analysis tracks proves that while gray cast iron remains a structurally reliable and inexpensive baseline material, it suffers from pronounced structural deformation and slower heat migration pathways. AlSiC MMCs circumvent the classic engineering trade-offs of lightweight alloys by utilizing ceramic particle reinforcement to match or exceed the structural stress capacity of cast iron, while fully exploiting the superior weight reduction and rapid thermal dissipation profiles characteristic of an Aluminium base [18].

9. Conclusion

A comparative CAD/FEA framework was used for cast iron and Al–SiC disc-brake rotor models. Under the reported conditions, Al–SiC showed lower total deformation and slightly lower equivalent stress than cast iron. Both materials showed a reported maximum temperature of 80 °C, while Al–SiC showed slightly higher heat-flux values. The pressure implied by the stated force and area is 9.1820 MPa; the alternative 17.178 MPa requires confirmation.. Al–SiC is identified only as a promising lightweight material requiring verified material data, mesh convergence, thermal/contact validation, wear assessment and experiments.

Conflict of Interest Statement: The author states that there is no conflict of interest in terms of this research, the analysis, or the preparation of this article for publication.

Funding Information: The author did not receive support from any organization for the submitted work.

Data Availability Statement: Required data are furbished in the article. The author may be contacted on reasonable request for any further information about the data.

Ethical Approval Statement: No experiments were undertaken with human participants, and this study was purely observational. No identifying, personal or sensitive information is reported.

Acknowledgement Section: The author wishes to acknowledge all his friends and students who follow his research articles through his Google Scholar page or other specialized sites. The author also thanks the Editors and Reviewers of IJDST for their time and engagement with this paper.

References

1. Chengal Reddy V, Gunasekhar Reddy M, Harinath Gowd G, Modeling and Analysis of FSAE Car Disc Brake Using FEM. 2013
2. Praveena S, Lava Kumar M, Sreekanth Reddy S, Modeling and Structural Analysis of Disc Brake. 2014
3. Lee S, Yeo T, Temperature and Coning Analysis of Brake Rotor Using an Axisymmetric Finite Element Technique. 2000
4. Belhocine A, Abu Bakar AR, Bouchetara M, Structural and Contact Analysis of Disc Brake Assembly During Single Stop Braking Event
5. Limpert R, Brake Design and Safety, 2nd ed., SAE. 1999
6. Komanduri R, Hou ZB, Analysis of Heat Partition and Temperature Distribution in Sliding Systems, Wear. 2001, (251):925-938
7. Jang YH, Ahn SH, Frictionally-Excited Thermoplastic Instability in Functionally Graded Naterial, Wear. 2007, (262):1102-1112
8. Dufrenoy P, Weichert D, A Thermo Mechanical Model for the Analysis of Disc Brake Fracture Mechanisms, Journal of Thermal Stresses. 2003, (26):815-828
9. Panier S, Dufrenoy P, Weichert D, An Experimental Investigation of Hot Spots in Railway Disc Brakes, Wear. 2004, (256):764-773
10. Kao TK, Richmond JW, Douarre A, Brake Dsc Hot Spotting and Thermal Judder: An Experimental and Finite Element Study, International Journal of Vehicle Design. 2000, (23):276-296
11. Kim DJ, Lee YM, Park JS, Seok CS, Thermal Stress Analysis for a Disk Brake of Railway Vehicles with Consideration of Pressure Distribution, Materials Science and Engineering A. 2008, (483–484):456–459
12. Bagnoli F, Dolce F, Bernabei M, Thermal Fatigue Cracks of Fire Fighting Vehicles Gray Iron Brake Discs, Engineering Failure Analysis. 2009, (16):152-163
13. Li W, Thermo Mechanical Fatigue Behavior of Spray-Deposited SiCp/Al-Si Composite Applied in the High-Speed Railway Brake Disc, International Journal of Photo Energy. 2020
14. Meng T, Effect of Grp on Microstructure and Properties of SiCp/Al Composites for Brake Discs, Tribology Transactions. 2021
15. Ferraris M, Gili F, Lizarralde X, Igartua A, Mendoza G, Blugan G, et al., SiC Particle Reinforced Al Matrix Composites Brazed on Aluminium Body for Lightweight Wear Resistant Brakes, Ceramics International. 2022, 48(8):10941-10951
16. Bahulekar A, Shiralkar S, Jomde A, Shamkuwar S, Patane P, Shinde T, et al., Structural and Thermal Analysis of Brake Disc with Various Composites, SAE Technical Paper. 2024, 28-0066
17. Hou G, Cui Y, Tribological Performance of Carbon/Silicon Carbide Brake Composite at High Temperature: Behaviors and Mechanisms, Ceramics International. 2024
18. Trinh PH, Thanh DV, Parametric Multi Scale Homogenization and Coupled Thermo-Structural Analysis of Hybrid Al-SiC-Gr Brake Discs Via Sequential Micromechanical Modeling, Journal of Composites Science. 2026